Am J Cancer Res 2023;13(12):6210-6225
www.ajcr.us /ISSN:2156-6976/ajcr0153871

Original Article

Estrogen receptor α inhibits Caveolin 1 translation by promoting m6A-dependent miR199a-5p maturation to confer nab-paclitaxel resistance

Jianping Zhang[1], Zhuo Wang[2], Liyuan Zhu[1], Chaoqun Wang[3], Bifei Huang[3], Yiming Zhong[1], Pingting Ying[1], Hanying Wang[2], Qinglin Li[4], Lifeng Feng[1], Xian Wang[2], Hongchuan Jin[1]

[1]Biomedical Research Center, Sir Run Run Shaw Hospital, School of Medicine, Zhejiang University, Hangzhou, Zhejiang, China; [2]Department of Medical Oncology, Sir Run Run Shaw Hospital, School of Medicine, Zhejiang University, Hangzhou, Zhejiang, China; [3]Department of Pathology, Affiliated Dongyang Hospital of Wenzhou Medical University, Dongyang, Zhejiang, China; [4]The Cancer Hospital of The University of Chinese Academy of Sciences, Hangzhou, Zhejiang, China

Received October 11, 2023; Accepted November 15, 2023; Epub December 15, 2023; Published December 30, 2023

Abstract: Estrogen receptor positive (ER+) breast cancer patients exhibit poorer responsiveness to nab-paclitaxel compared to ER negative (ER-) patients, with the underlying mechanisms remaining unknown. Caveolin 1 (CAV1) is a membrane invagination protein critical for the endocytosis of macromolecules including albumin-bound chemotherapeutic agents. Here, we demonstrate that ERα limits the efficacy of nab-paclitaxel in breast cancer cells while genetic or pharmacological inhibition of ERα increased the sensitivity of ER+ breast cancer cells to nab-paclitaxel. Notably, CAV1 expression inversely correlates with ERα and relates to improved clinical outcomes from nab-paclitaxel treatment. Importantly, ERα stimulates m6A dependent maturation of miR199a-5p, which is elevated in ER+ breast cancer, to inhibit CAV1 translation by antagonizing m6A modification of CAV1 mRNA. Together, our findings reveal a novel role of ERα in promoting m6A modification and subsequent maturation of miR199a-5p, which is upregulated in ER+ breast cancer, leading to the suppression of m6A modification of CAV1 and its mRNA translation, thereby contributing to nab-paclitaxel resistance. Thus, combining an ER antagonist with nab-paclitaxel could offer a promising strategy for treating ER+ breast cancer patients.

Keywords: Estrogen receptor α (ERα), nab-paclitaxel, Caveolin 1 (CAV1), translation, N6-methyladenosine (m6A), miR199a-5p

Introduction

Estrogen receptor α (ERα) drives approximately 75% of breast cancers (BC) and is often treated with routine endocrine therapy [1, 2]. Despite this, many ER+ BC patients experience relapse post-treatment, necessitating chemotherapy in recurrent or metastatic stages [3]. Nab-paclitaxel (Abraxane), the first clinically successful albumin-bound chemotherapeutic agent (paclitaxel linked to human albumin), is widely used in the treatment of pancreatic cancer, non-small cell lung cancer (NSCLC), and breast cancer [4-6]. However, some clinical trials and retrospective analyses have observed that nab-paclitaxel is less effective in ER+ BC than in ER- BC [7], suggesting that ER status may play an important role in nab-paclitaxel response, despite a lack of understanding of the underlying mechanisms.

Caveolin 1 (CAV1) is the principal structural protein of Caveolae, which are 50-100 nm flask-shaped invaginations of the plasma membrane crucial for endocytosis, cholesterol homeostasis, signal transduction, and macromolecule transport [8]. CAV1 is reported to be upregulated in pancreatic cancer, NSCLC, and breast cancer, and has been implicated in increased invasion, metastasis, resistance to radiation or chemotherapy, and poor prognosis [9, 10]. In addition, a previous study claimed that CAV1 is an albumin transporter that facilitates nab-paclitaxel uptake to enhance its efficacy in pan-

creatic cancer and NSCLC [8]. However, the relevance of CAV1 to nab-paclitaxel resistance in ER+ BC remains unknown.

In this study, we demonstrate that ERα mediates nab-paclitaxel resistance by inhibiting CAV1 translation. Mechanistically, ERα fosters m6A-dependent maturation of miR199a-5p, which binds to CAV1 mRNA, thereby competitively suppressing m6A modification and subsequent translation. Our study provides a compelling rationale for targeting ERα to overcome nab-paclitaxel resistance in ER+ breast cancer.

Methods and materials

Patients and retrospective study design

A cohort of 116 breast cancer patients who received nab-paclitaxel at Sir Run Run Shaw Hospital, Zhejiang University, between January 2008 and May 2022 were retrospectively reviewed. All eligible patients received at least one dose of nab-paclitaxel. We analyzed the baseline ER status by IHC and evaluated disease progression using the RECIST guidelines [11].

Cell lines, antibodies and reagents

The breast cancer cell lines MCF-7, T-47D, MB231, and BT549 were purchased from the American Type Culture Collection (ATCC). Both were authenticated using short tandem repeat multi-amplification and tested negative for Mycoplasma. MCF-7 and T-47D cells were cultured in DMEM (Gibco, USA), and MB231 and BT549 cells were cultured in RPMI-1640 medium (Gibco, USA) supplemented with 10% FBS (Hyclone, USA), 100 U/ml penicillin, and 100 μg/ml streptomycin (Life Technologies/Gibco, Shanghai, China). Cells were grown at 37°C in a humidified incubator with 5% CO_2 and 95% humidity.

The following antibodies were used for western blotting or immunohistochemistry: ERα (Vector Laboratories, VP-E613), CAV1 (ABclonal, A1555), METTL3 (ABclonal, A8370), β-actin (Cell Signaling Technology, 4970), Cleaved PARP1 (C-PARP1) (Cell Signaling Technology, 9541), Cleaved Caspase-3 (Cell Signaling Technology, 9661), 4-OH-Tamoxifen (579002), and β-estradiol (E8875) were purchased from Merck and Sigma Aldrich. Fulvestrant (HY-13636) was purchased from MedChemExpress (Shanghai, China). Nab-paclitaxel was supported by the Celgene Corporation. DQ™ Green BSA (Invitrogen™, 1014496).

SiRNA, miRNA mimics/inhibitors and plasmid transfections

Small interfering RNA (siRNA) targeting ERα, CAV1, METTL3, and microRNAs were synthesized by GenePharma (Shanghai, China) and RiboBio (Guangzhou, China). The sequences of the siRNAs and miRNA mimics/inhibitors are listed in Table S1. The plasmids Flag-CAV1-pcDNA3.1 and Flag-ERα-pcDNA3.1 were purchased from Genechem (Shanghai, China). SiRNAs and miRNA mimics/inhibitors were transfected into cells seeded overnight using lipo2000 (Invitrogen, USA) or Lipofectamine RNAiMax transfection reagent (Invitrogen, USA) according to the manufacturer's instructions.

RNA extraction, reverse transcription and qPCR

Total RNA was extracted using TRIzol reagent (Invitrogen, 15596026) according to the manufacturer's instructions, and RNA concentration was quantified using a NanoDrop 2000 (Nanodrop, Wilmington, DE, USA). RNA (1-2 μg) was reverse-transcribed using the High Capacity cDNA Reverse Transcription Kit (Thermo Fisher Scientific, 4368813). Real-time PCR (qPCR) was conducted using a SYBR Green Master Mix Kit (ComWin Biotech, CW0659s, Beijing, China). The qPCR data were normalized to the control group, and the relative expression of the indicated genes shown in the histograms is expressed as mean ± SD. The primers used in this study are listed in Table S1.

Luciferase activity assay

The fragment of the CAV1 3'-UTR containing the miR-199a-5p binding site was amplified by PCR. and was inserted into the pMIR-REPORT Luciferase (Promega). For the luciferase assay, HEK-293T in 6-well plates. The CAV1-3'UTR plasmids were co-transfected using lipo2000 with miR199a-5p mimics and pRL Renilla as an internal control (Invitrogen, USA). After 48 h, the luciferase activity was measured using the Dual-GLO Luciferase Assay System (Promega Corporation, USA).

RNA immunoprecipitation (RIP) assay

The RIP assay was conducted following the manufacturer's instructions for the Magna RIP™ RNA-Binding Protein Immunoprecipitation Kit (Millipore, No. 17-700). Cells (> 2 × 10^7) were collected and lysed in 100 μl RIP lysis buffer, immunoprecipitated with the indicated antibody-linked beads or protein G magnetic beads overnight at 4°C, washed six times in Washing Buffer, and the protein was denatured at 55°C. Total RNA was isolated and quantified using RT-PCR analysis.

Puromycin-labelling

5 × 10^6 cells were plated in a 10 cm dish and incubated with 1:1000 biotin-dC-puromycin (NU-925-BIO-S, Jena Bioscience) for 24 h. Cells were collected and lysed in 1% NP40 buffer with protease inhibitor cocktail. After 15000 rpm × 30 min centrifugation at 4°C, the supernatant was collected and incubated with 80 ul streptavidin sepharose beads (GE17-5113-01, Sigma) by rotating at 4°C overnight. The mixture was washed five times with 1% NP40 buffer for 5 times and test CAV1 expression was tested by western blotting.

Biotin pull down assay

Cells were transfected with biotinylated miR199a-5p probes for 48 h and resuspended in lysis buffer (20 mM Tris, pH 7.5, 200 mM NaCl, 2.5 mM $MgCl_2$, 60 U/mL SUPERase-In, 1 mM DTT, 0.05% Igepal, protease inhibitors). Lysates were incubated with prepared streptavidin beads (GE Healthcare). Yeast tRNA (Sigma-Aldrich) was used to block the lysates at 4°C for 3 h. The cells were washed five times with binding and wash buffer (5 mM Tris-HCl, pH 7.5, 0.5 mM EDTA, 1 M NaCl). Finally, the bound RNAs was extracted and purified for qPCR.

In vitro pri-miRNA processing assays

Probe biotin-pri-miR-199 was transcribed in vitro using a T7 based MEGA shortscript kit (Life Technologies). Biotin RNA-labeling Mix (Roche, 11685597910) was used for the in vitro transcription reaction. For pri-miR-199 processing assays, biotin-pri-miR-199 was incubated with whole cell lysates of 293T cells at 37°C for 90 min. The Lysates were then incubated with streptavidin beads (GE Healthcare). RNA purified from the reaction products was analyzed by qRT-PCR. The primers used for in vitro pri-miR-199 transcription are listed in Table S1.

Animal experiments

Six-week-old female BALB/c nude mice from the Center of Experimentation of Zhejiang University were used following the Institutional Animal Care and Use Committee and National Institute of Health (NIH) guidelines. Tumors were established by subcutaneous injection (1 × 10^6 E0771 cells in 0.1 ml saline) into the flanks of the mice. After 12 days, tumors reached > 150 mm^3 in size, and the mice were randomly allocated into four groups and treated with Nab-PTX (22.3 mg/kg body weight; i.p., every 3 days), Fulvestrant (2.5 mg/kg body weight; i.p., every 3 days), Nab-PTX combined with fulvestrant, or vehicle PBS as control. Tumor volume was measured every 3 days. Mice were euthanized when the tumor size reached approximately 2000 mm^3. Tumor volume was calculated using the following formula: length × $width^2$ × 0.5.

Statistical analysis

All data are presented as mean ± SD. The statistical approach used in every experiment to compare the differences between the groups is provided in the figure legends. Statistical significance was set at $P < 0.05$.

Results

ER+ BC patients exhibit a worse response to nab-paclitaxel compared to ER- BC patients

To evaluate if ER status influences responsiveness to nab-paclitaxel, we retrospectively reviewed a cohort of 116 breast cancer patients who received nab-paclitaxel at Sir Run Run Shaw Hospital, Zhejiang University, between January 2008 and May 2022. All eligible patients received at least one dose of nab-paclitaxel (**Figure 1A**). We analyzed baseline ER status to predict disease progression, according to the RECIST guidelines. Of the patients, 55 (64.7%) were classified as ER-positive, and 30 (35.2%) were classified as ER-negative (Figure S1). In the ER+ subgroup, 4 patients (7.3%) achieved partial response

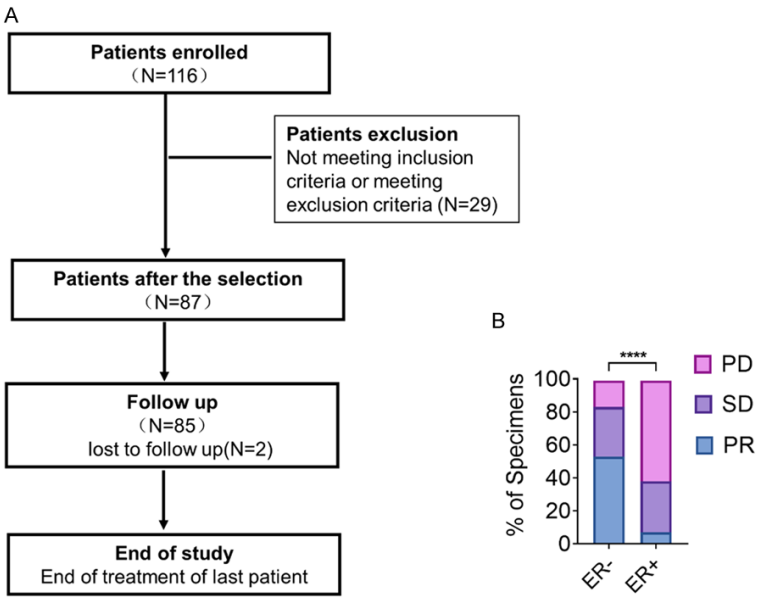

Figure 1. Lower response to Nab-paclitaxel in ER+ BC than ER- BC. A. Work flow of patient enrollment and responses. B. Therapeutic evaluation in ER+ and ER- BC patients.

(PR), 17 (30.9%) had stable disease (SD), and 34 (61.8%) experienced disease progression (PD). Conversely, in the ER- group, 16 patients (53.3%) achieved PR, 9 (30%) had SD, and 5 (16.7%) experienced PD. There was a significant difference in the objective response rate (ORR) and disease control rate (DCR) between these groups (**Figure 1B**), consistent with previous reports [7].

ER+ BC is less sensitive to nab-paclitaxel than ER- BC in vitro

In vitro, ERα-BC cells (MB231 and BT549) displayed lower viability post-nab-paclitaxel treatment than ERα+ cells (MCF7 and T47D) (**Figure 2A**, **2B**). Furthermore, equivalent doses of nab-paclitaxel induced more apoptosis in ERα-BC cells (MB231 and BT549) than ERα+BC cells (MCF7 and T47D) (**Figure 2C**). Moreover, MCF7 (ER+) and MB231 (ER-) cells exhibited similar sensitivity to paclitaxel (**Figure 2D**). However, equivalent doses of nab-paclitaxel displayed superior efficacy to paclitaxel, while MB231 cells but not MCF7 cells were much more sensitive to nab-paclitaxel than paclitaxel (**Figure 2E**). Collectively, these findings indicate that ER+ BC respond less effectively to nab-paclitaxel than ER- BC.

ERα inhibits the sensitivity of breast cancer cells to nab-paclitaxel

Given the distinct response to nab-paclitaxel in ER+ and ER- breast cancers, we questioned whether ERα inhibits the anticancer activity of nab-paclitaxel. Indeed, genetic knockdown of ERα in MCF7 cells, combined with nab-paclitaxel, significantly suppressed cell proliferation (**Figure 3A**), upregulated apoptosis (**Figures 3B**, **3C** and S2A) compared to nab-paclitaxel alone. Similarly, chemical inhibition of ERα by Tamoxifen and Fulvestrant in MCF7 and T47D cells greatly enhanced the growth-inhibitory effects of nab-paclitaxel, suggesting that ERα inhibition enhances nab-paclitaxel anticancer activity (**Figures 3D-I** and S2B-E). Furthermore, β-estradiol (β-E2) deprivation amplified the inhibitory effect of nab-paclitaxel on cell proliferation (**Figure 3J**), reduced colony formation (**Figure 3K**), and activated apoptosis (**Figure 3L**), while β-E2 supplementation attenuated this effects. In contrast, fulvestrant did not influence the sensitivity of MCF7 cells to paclitaxel (**Figure 3M**), indicating a potential connection to nab-paclitaxel uptake. Altogether, these results suggest that ERα reduces the sensitivity of breast cancer cells to nab-paclitaxel, with a possible mechanism driven by modification of nab-paclitaxel uptake.

CAV1 is relevant to the sensitivity of breast cancer cells to nab-paclitaxel

As CAV1 is critical for the response to albumin-bound chemotherapeutics in Non-Small Cell Lung Cancer (NSCLC) and pancreatic cancer by affecting albumin endocytosis [8], we assessed the effect of CAV1 on nab-paclitaxel sensitivity in breast cancer cells. After siRNA-mediated CAV1 knockdown, MB231 and BT549 cells displayed resistance to nab-paclitaxel (**Figures 4A**, S3A-C). Conversely, expressing exogenous CAV1 in MCF7 and T47D cells

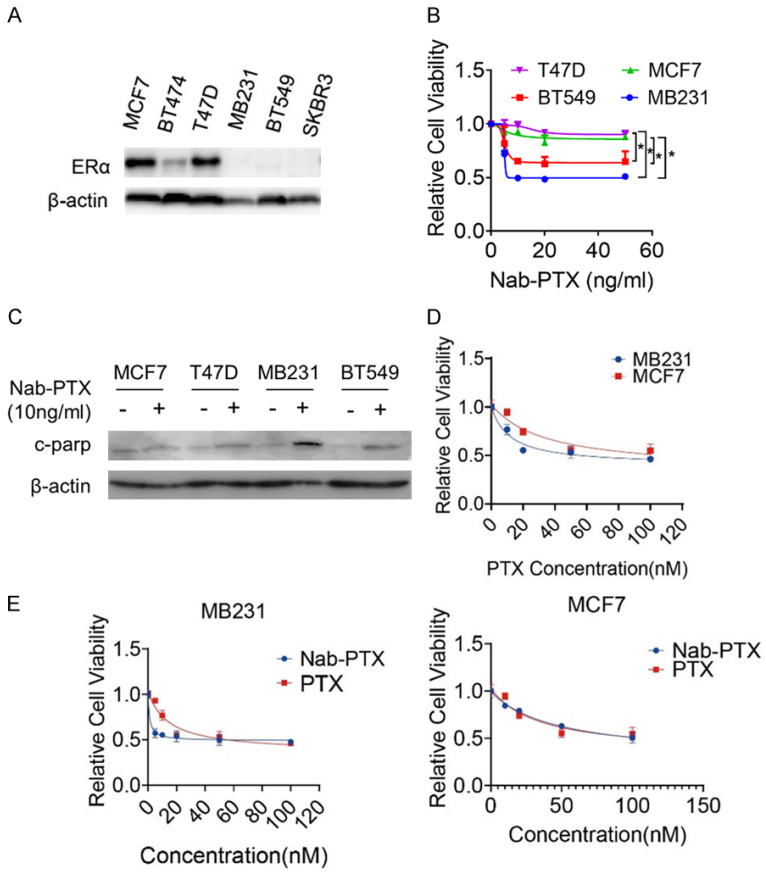

Figure 2. ER+ BC is less sensitive to nab-paclitaxel than ER- BC in vitro. A. ER status test by Western blot. B. Analysis of cell viability in ER+ BC (MCF7 and T47D) and ER- BC (MB231 and BT549) with Nab-PTX treatment by MTS assays. C. Analysis of apoptosis in ER+ BC (MCF7 and T47D) and ER- BC (MB231 and BT549) with or without Nab-PTX treatment by western blot. D. Analysis of cell viability in MCF7 and MB231 with paclitaxel treatment by MTS assays. E. Nab-paclitaxel and paclitaxel distinct sensitivity in MCF7 and MB231 T test was performed for significant analysis, significant difference is indicated with * for $P < 0.05$.

increased their sensitivity to nab-paclitaxel (**Figures 4B**, S3D, S3E). However, their sensitivity to paclitaxel remained unchanged regardless of CAV1 knockdown or overexpression (**Figure 4C**, **4D**), suggesting a role for CAV1 in mediating the internalization of albumin-bound drugs. Indeed, DQ-BSA encapsulation for 30 minutes in culture medium [12], led to high cytoplasmic accumulation in MB231 cells, which was abrogated following CAV1 knockdown (**Figure 4E**). Notably, patients with higher CAV1 expression benefited more from nab-paclitaxel treatment (**Figure 4F**), indicating a positive correlation between CAV1 expression and disease control rate in breast cancer post nab-paclitaxel treatment. In conclusion, CAV1 expression plays a significant role in determining the response to nab-paclitaxel.

ERα downregulates CAV1 protein expression by inhibiting its translation

To explore the potential correlation between ERα and CAV1, we analyzed their expression using reverse-phase protein arrays (RPPA) (n=627) from The Cancer Proteome Atlas (TCPA) database. There was a significant negative correlation between CAV1 and ERα protein levels (**Figure 5A**). However, no correlation was observed between CAV1 and ESR1 mRNA levels based on results from The Cancer Genome Atlas (TCGA) (Figure S4A). Additionally, CAV1 protein expression was much lower in ERα-positive breast cancer tissues compared to ERα-negative (**Figure 5B**, **5C**). Moreover, CAV1 protein levels were notably higher in ERα-negative breast cancer cell lines than in ERα-positive breast cancer cell lines (**Figure 5D**). Following ERα knockdown with siRNA or treatment with ERα inhibitors (4-OH-Tamoxifen and Fulvestrant), CAV1 protein was upregulated (**Figures 5E**, **5F** and S4B-D) whereas CAV1 mRNA remained constant (Figure S4E-G). In contrast, exogenous ERα overexpression or ER activation by 17β-E2 inhibited CAV1 protein expression while CAV1 mRNA remained constant (**Figures 5F**, **5G** and S4H). Moreover, ERα inhibition or activation did not alter the expression of exogenously introduced CAV1, which lacks a 3'UTR (Figure S4I, S4J). What's more, ER inhibitor Fulvestrant treatment doesn't change the CAV1 protein degradation (Figure S4K). These findings suggest that ERα inhibits CAV1 translation. In fact, nascent CAV1 protein synthesis increased with ERα depletion, either by siRNA or chemical inhibition with fulvestrant (**Figure 5H**, **5I**). Thus, ERα downregulates CAV1

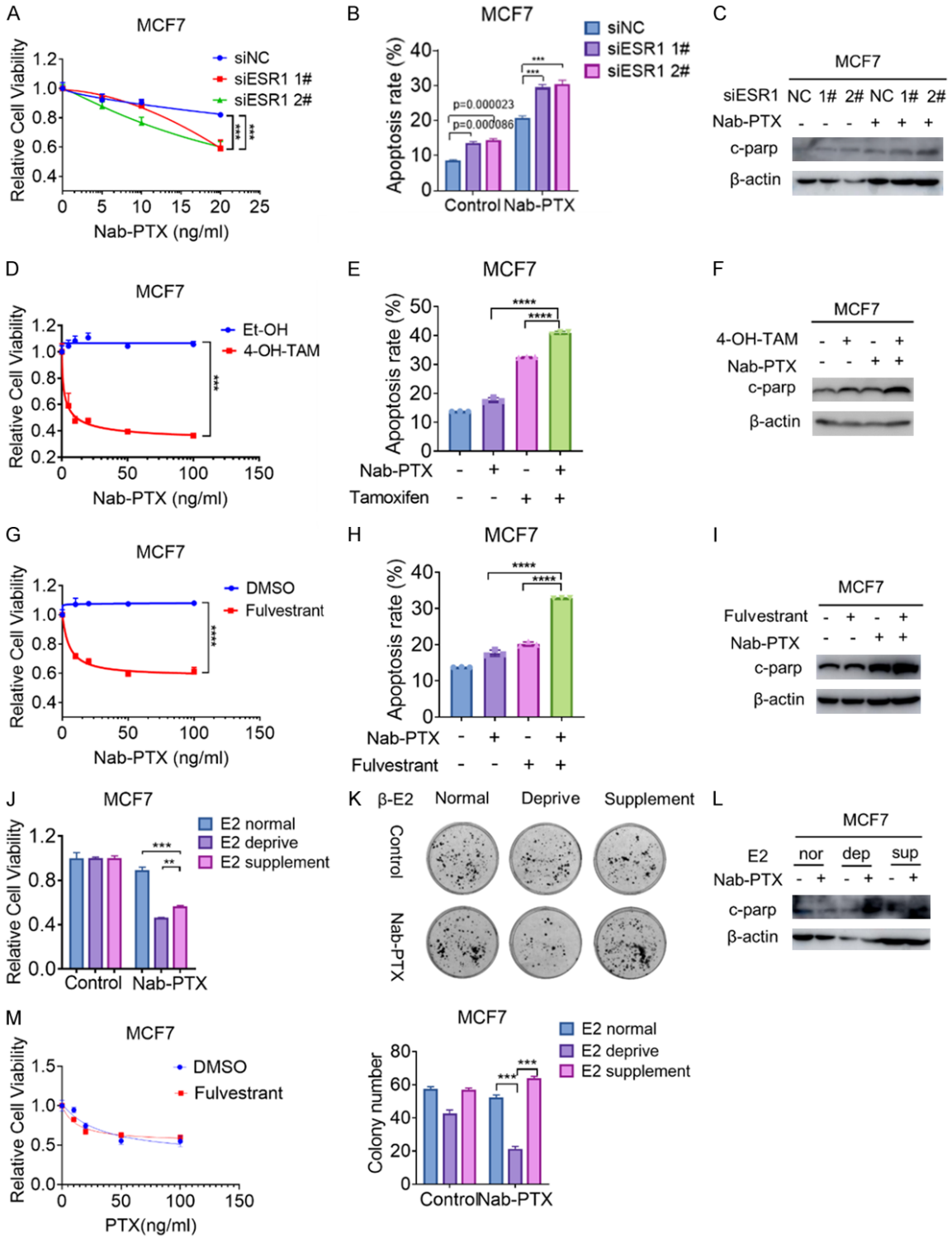

Figure 3. Inhibition of ERα enhance the sensitivity to Nab-paclitaxel in vitro. A. Analysis of cell viability after siESR1 with Nab-PTX in MCF7 cells using MTS assay. B. Analysis of cell viability after siESR1 with Nab-PTX in MCF7 cells using flow cytometry. C. Analysis of cell apoptosis after siESR1 with Nab-PTX in MCF7 cells through Western blot. D. Analysis of cell viability after combining 4-OH-TAM (5 uM) with Nab-PTX in MCF7 cells using MTS assays. E. Analysis of cell viability after combining 4-OH-TAM (5 uM) with Nab-PTX in MCF7 cells using flow cytometry. F. Analysis of cell apoptosis after combining 4-OH-TAM (5 uM) with Nab-PTX in MCF7 cells using Western blot. G. Analysis of cell viability after combining Fulvestrant (100 nM) with Nab-PTX in MCF7 cells using MTS assays. H. Analysis of cell viability after combining Fulvestrant (100 nM) with Nab-PTX in MCF7 cells using flow cytometry. I. Analysis of cell apoptosis

after combining Fulvestrant (100 nM) with Nab-PTX in MCF7 cells using Western blot. J. Analysis of cell viability before and after β-E2 treatment with Nab-PTX in MCF7 cells by MTS assays. K. Analysis of cell viability before and after β-E2 (5 nM) treatment with Nab-PTX in MCF7 cells using colony formation. L. Analysis of cell apoptosis before and after β-E2 (5 nM) treatment with Nab-PTX in MCF7 cells using Western blot. M. Analysis of cell viability combining Fulvestrant with paclitaxel by MTS assays.

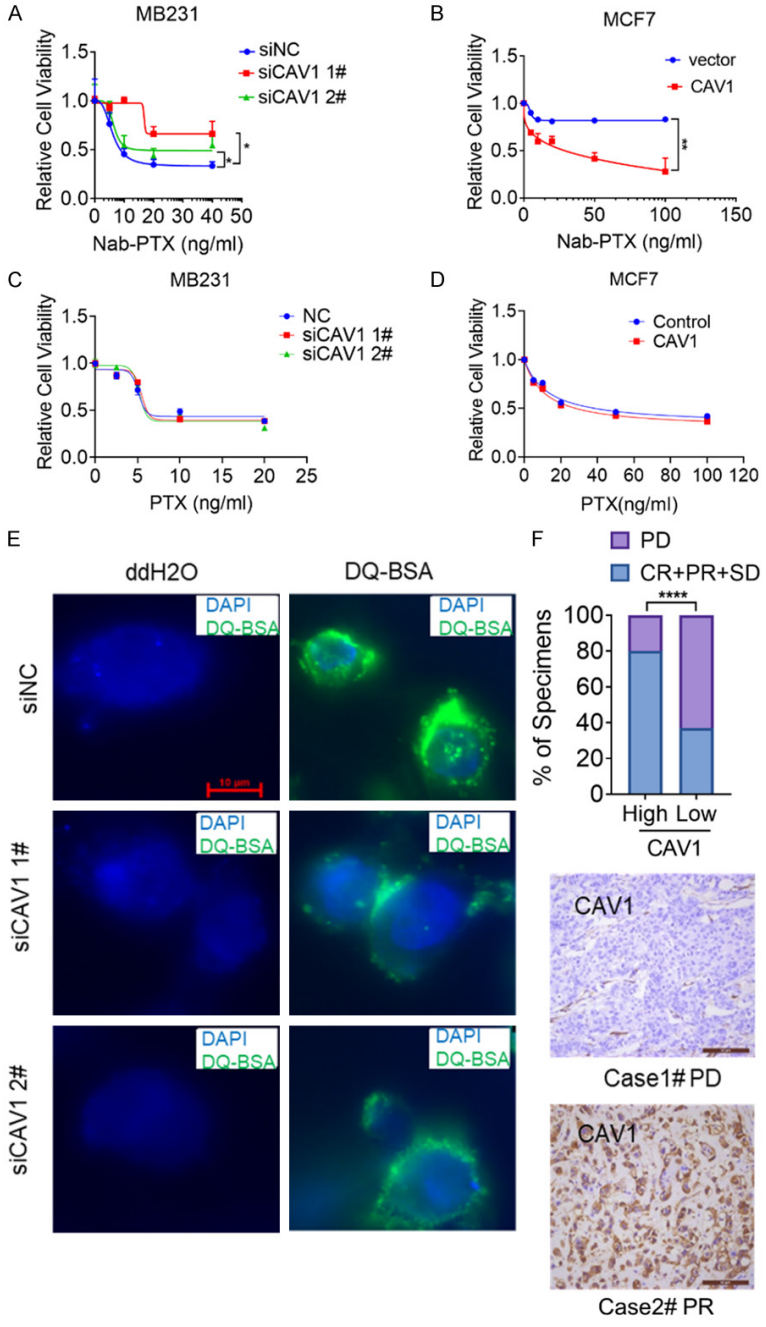

Figure 4. CAV1 is relevant to the sensitivity of breast cancer cells to Nab-paclitaxel. A. Analysis of cell viability after siCAV1 with Nab-PTX in MB231 cells using MTS assay. B. Analysis of cell viability after overexpression of CAV1 with Nab-PTX in MCF7 cells by the MTS assay. C. Analysis of cell viability after siCAV1 with PTX in MB231 cells by the MTS assay. D. Analysis of cell viability after overexpression of CAV1 with PTX in MCF7 cells by the MTS assay. E. Immunofluorescence after siCAV1 with DQ-BSA encapsulated for 30 min in MB231 cells. F. Immunohistochemical analysis of CAV1 protein expression in Nab-PTX-treated patients.

expression by inhibiting its translation.

ERα upregulates miR199a-5p to inhibit m6A modification of CAV1

MicroRNAs (miRNAs) are widely recognized as negative regulators of protein translation through partial base-pairing with the 3'-UTR of mRNA to block formation of the translation initiation complex [13-15]. Furthermore, N6-methyladenosine (m6A) modification has also been found to play a critical role in regulating protein translation [16, 17]. However, whether these two post-transcriptional modifications have interplay remains unknow. Thus, we queried potential miRNAs upregulated upon E2 stimulation (data from GSE78167) and predicted target CAV1 using TargetScan, miRDB, and StarBase. This analysis revealed seven overlapping miRNAs: hsa-miR-493-3p, hsa-miR-520a*, hsa-miR-384, hsa-miR-124-3p, hsa-miR-512-3p, hsa-miR-199a-5p, and hsa-miR-302b* (**Figure 6A**). Inhibition of miR-199a-5p, miR-512-3p, or miR-520a, but not of other miRNAs, upregulated CAV1 protein levels (**Figure 6B**). Furthermore, knockdown of ERα downregulated the expression of only two miRNAs, miR-124-3p and miR-199a-5p (**Figure 6C**). We therefore postulated that miR-199a-5p may be involved in the ERα-mediated regulation of CAV1 protein translation. Indeed, a miR-199a-5p mimic reduced CAV1 protein expression while its

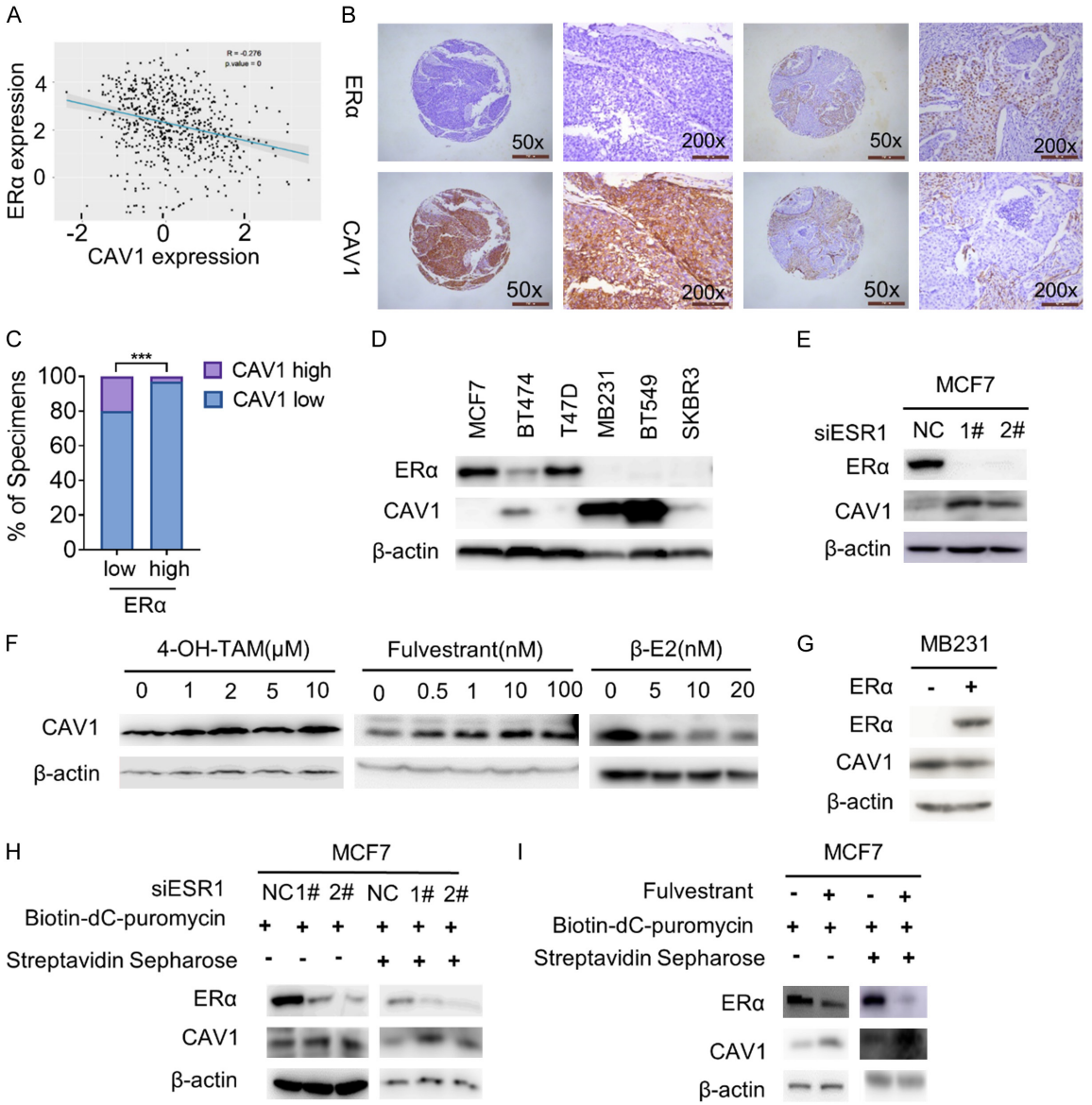

Figure 5. ERα downregulates CAV1 protein expression by inhibiting its translation. A. Correlation between ERα and CAV1 mRNA levels in BC tissues from TCPA. B and C. IHC analysis of the association between CAV1 and ERα protein expression in BC tissues. D. Western blot analysis of CAV1 and ERα expression in different BC cell lines. E. Western blot analysis of CAV1 protein expression after siESR1 treatment in MCF7 cells. F. Western blot analysis of CAV1 protein expression after treatment with 4-OH-TAM, fulvestrant, or β-E2 in MCF7 cells. G. Western blot analysis of CAV1 protein expression after ERα overexpression in MB231. H and I. Puromycin-labelling test for CAV1 translation after siESR1 or fulvestrant treatment in MCF7 cells.

inhibition increased protein expression (**Figure 6D**). Additionally, luciferase activity driven by the CAV1 mRNA 3'-UTR was significantly inhibited by miR199a-5p (**Figure 6E**). The interaction between miR199a-5p and CAV1 mRNA was further confirmed by a biotin pulldown assay (**Figure 6F**). Importantly, the miR-199a-5p mimic succeeded in rescuing CAV1 upregulation induced by fulvestrant (Figure S5A), emphasizing the role of miR199a-5p upregulation to ERα-mediated CAV1 downregulation.

Next, we analyzed the meRIP-Seq data, revealing a hypermethylated peak in the 3'-UTR of CAV1 mRNA (Figure S5B). m6A modification of CAV1 mRNA was confirmed by RIP-qPCR (**Figure 6G**). The m6A writer METTL3 was also found to bind to CAV1 mRNA (Figure S5C). METTL3

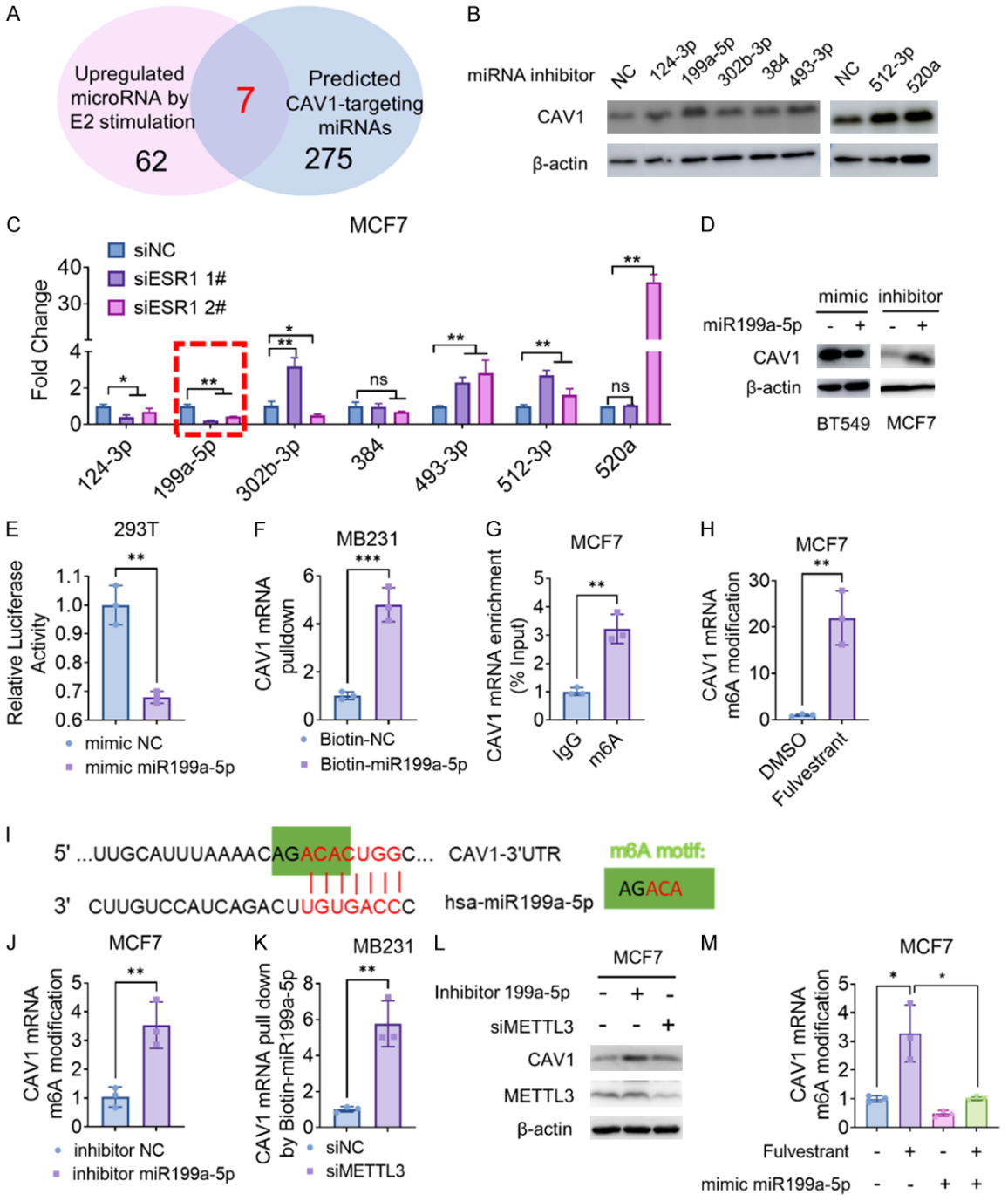

Figure 6. ERα upregulates miR199a-5p to inhibit m6A modification of CAV1. A. Venn diagram: miRNAs upregulated by E2 stimulate VS predicted CAV1-targeting miRNAs. B. Western blot analysis of CAV1 protein expression after treatment with the miRNA inhibitor. C. Real-time PCR analysis of CAV1 mRNA levels after siESR1. D. Western blot analysis of CAV1 protein expression after mimic miR199a-5p and inhibitor miR199a-5p. E. Luciferase assay analysis of miR199a-5p binding ability to CAV1. F. RNA pull-down analysis miR199a-5p binding ability to CAV1. G. RIP analysis of CAV1 m6A modification. H. RIP analysis CAV1 m6A level after fulvestrant treatment. I. miR199a-5p seed region overlap CAV1 3'UTR m6A motif "AGACA". J. RIP analysis of CAV1 m6A modification after miR199a-5p inhibition. K. RNA pull-down analysis of miR199a-5p bind to the CAV1 3'UTR after siMETTL3. L. Western blot analysis CAV1 expression after miR199a-5p inhibition and rescued by siMETTL3. M. RIP analysis of CAV1 m6A modification after miR199a-5p inhibition and rescue by fulvestrant.

knockdown effectively reduced m6A modification of CAV1 mRNA (Figure S5D), accompanied by decreased synthesis of nascent CAV1 protein (Figure S5E). Thus, METTL3-mediated m6A modification is crucial for efficient translation of CAV1 mRNA. Importantly, inhibition of ERα by fulvestrant increased both m6A modification and METTL3 binding to CAV1 mRNA (**Figures 6H** and S5F). Furthermore, the upregulation of CAV1 protein expression induced by ERα inhibition was reversed by METTL3 knockdown (Figure S5G), highlighting the dependence of ERα-regulated CAV1 protein translation on METTL3-mediated m6A modification. Interestingly, the seed sequence of the miR-199a-5p interaction contained a classical RRACH motif (AGACA) with potential for m6A modification (**Figure 6I**), suggesting that miR-199a-5p might counteract m6A modification to inhibit CAV1 translation. Indeed, the miR-199a-5p inhibitor increased CAV1 mRNA m6A levels (**Figure 6J**). Interestingly, miR-199a-5p was bound to the 3'UTR of CAV1 upon knockdown of METTL3 (**Figure 6K**), knockdown of METTL3 mitigated the CAV1 upregulation caused by miR199a-5p inhibition (**Figure 6L**), while the miR-199a-5p mimic rescued the fulvestrant-induced increase in m6A modification (**Figure 6M**), this indicates a competitive interplay between miR-199a-5p interaction and m6A modification of CAV1 mRNA. In summary, upregulated miR199a-5p antagonizes m6A modification to inhibit CAV1 translation.

ERα promotes m6A-dependent maturation of miR199a-5p

The expression of miR199a-5p positively correlates with ERα expression in breast cancer tissues (**Figure 7A**). Notably, miR199a-5p was highly expressed in ERα+ MCF7 cell but not ERα- cell MB231 (**Figure 7B**). Furthermore, inhibition of ERα by fulvestrant decreases mature miR-199a-5p and its precursor miR-199a, but increases primary miR-199a levels (**Figure 7C**), suggesting that ERα stimulates miR-199a-5p maturation. To confirm the effect of ERα on miR199a-5p maturation, we performed an in vitro RNA processing assay using in vitro-transcribed pri-miR199 incubated with whole-cell lysate pre- and post-fulvestrant treatment. ERα inhibition resulted in reduced conversion of pre-miR199 from pri-miR199 (**Figure 7D**). DGCR8 is a critical component of the microprocessor complex by participating in the cropping of pri-miRNAs into hairpin intermediates (pre-miRNAs). Indeed, DGCR8 interacts with pri-miR199a (Figure S6A) and knockdown of DGCR8 leads to accumulation of unprocessed pri-miR199 and decreased pre-miR199 generation (Figure S6B and S6C). Intriguingly, inhibition of ERα by fulvestrant diminishes the interaction between DGCR8 and pri-miR199 (**Figure 7E**), indicating that ERα enhances miR199a-5p maturation by modulating the interaction between DGCR8 and pri-miR199.

Recent studies have highlighted the crucial role of m6A modification in various miRNA maturations [18-20]. Classical m6A motifs are present in pri-miR199 (Figure S6D), m6A modification of pri-miR199 was confirmed by me-RIP (**Figure 7F**). Importantly, inhibition of m6A by METTL3 knockdown effectively downregulated the interaction of DGCR8 with pri-miR199 (**Figures 7G** and S6E), and hampers the biogenesis of mature miR199a-5p and pre-miR199 from pri-miR199 (**Figure 7H**), indicating that m6A modification is critical for the processing of pri-miR199.

Interestingly, inhibition of ERα reduces both the m6A modification of pri-miR199 and its interaction with METTL3 (**Figure 7I**, **7J**). Both ERα and METTL3 can interact with pri-miR199 (**Figure 7K**, **7L**). Moreover, ERα interacts with METTL3 (Figure S6F), implying that ERα may recruit METTL3 to facilitate m6A modification and subsequent processing of pri-miR199. In conclusion, ERα stimulates the m6A-dependent maturation of miR199a-5p.

Fulvestrant has a synergistic effect with nab-paclitaxel in ER+ breast cancer

Based on the mechanism identified above, we explored the clinical prospects of ERα inhibitors combined with Nab-paclitaxel in ER+ breast cancer patients. This hypothesis was first tested in a xenograft model using the ER+ murine breast cancer cell line, E0771 [21, 22] (**Figures 8A** and S7A-C). Twelve days post subcutaneous injection, nude mice were randomized to receive vehicle, fulvestrant alone (2.5 mg/kg), nab-paclitaxel alone (22.3 mg/kg), or a combination of fulvestrant and nab-paclitaxel. The combination treatment significantly delayed tumor growth, as evidenced by tumor volume and weight measurements (**Figures 8B**,

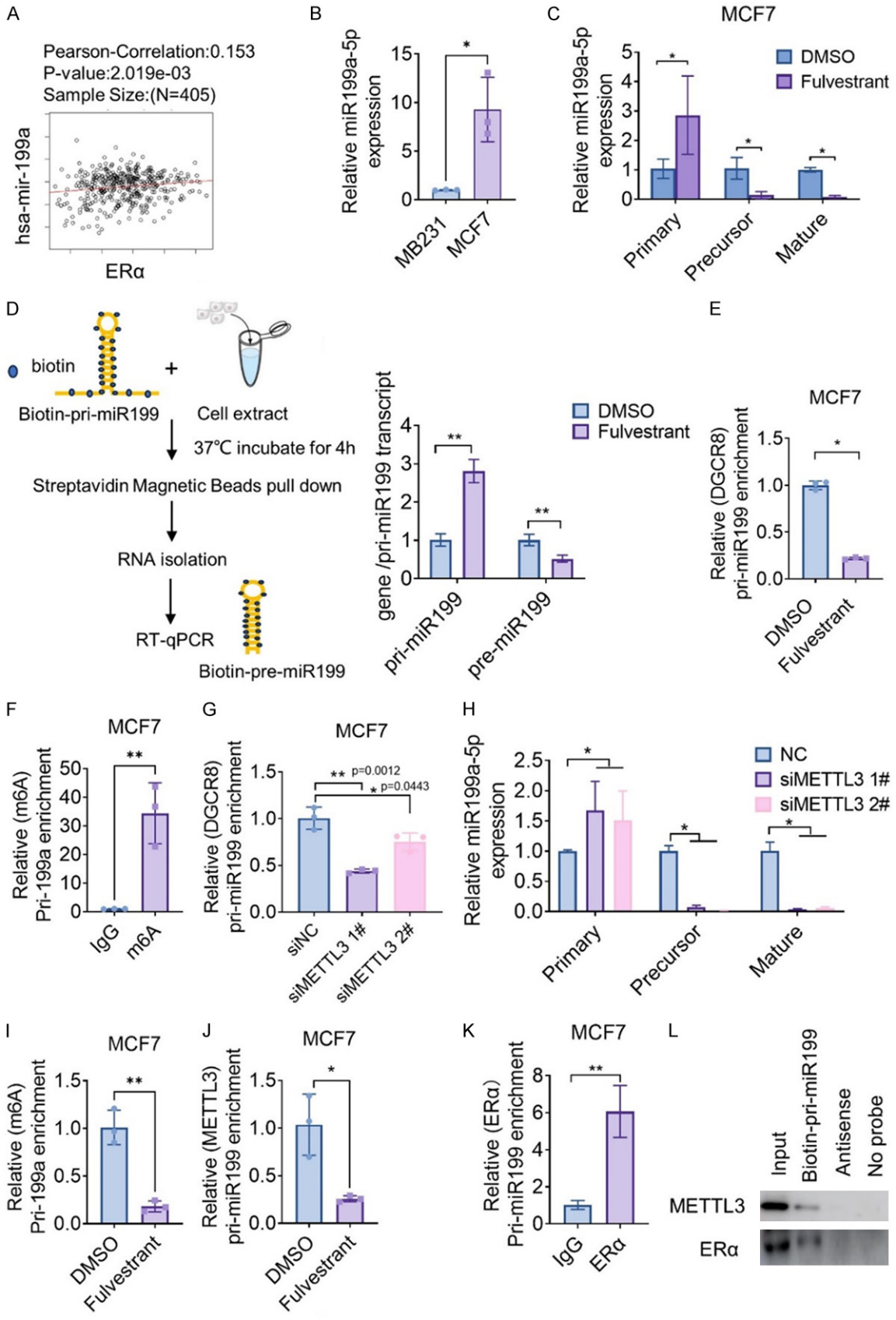
A
Pearson-Correlation:0.153
P-value:2.019e-03
Sample Size:(N=405)
hsa-mir-199a
ERα
B
Relative miR199a-5p expression
MB231
MCF7
C
MCF7
DMSO
Fulvestrant
Relative miR199a-5p expression
Primary
Precursor
Mature
D
biotin
Biotin-pri-miR199
Cell extract
37℃ incubate for 4h
Streptavidin Magnetic Beads pull down
RNA isolation
RT-qPCR
Biotin-pre-miR199
gene /pri-miR199 transcript
DMSO
Fulvestrant
pri-miR199
pre-miR199
E
MCF7
Relative (DGCR8) pri-miR199 enrichment
DMSO
Fulvestrant
F
MCF7
Relative (m6A) Pri-199a enrichment
IgG
m6A
G
MCF7
Relative (DGCR8) pri-miR199 enrichment
p=0.0012
p=0.0443
siNC
siMETTL3 1#
siMETTL3 2#
H
Relative miR199a-5p expression
NC
siMETTL3 1#
siMETTL3 2#
Primary
Precursor
Mature
I
MCF7
Relative (m6A) Pri-199a enrichment
DMSO
Fulvestrant
J
MCF7
Relative (METTL3) pri-miR199 enrichment
DMSO
Fulvestrant
K
MCF7
Relative (ERα) Pri-miR199 enrichment
IgG
ERα
L
Input
Biotin-pri-miR199
Antisense
No probe
METTL3
ERα

Figure 7. ERα promotes m6A-dependent maturation of miR199a-5p. A. Correlation between miR199a-5p and ERα protein. B. Real-time PCR analysis of miR199a-5p levels in MB231 and MCF7 cells. C. Real-time PCR analysis of pri-miR199, pre-miR199, and mature miR199a-5p expression in MCF7 cells before and after fulvestrant treatment. D. In vitro RNA processing assay analysis of pri-miR199 processing in lysates of MCF7 cells with or without fulvestrant treatment. E. RIP analysis of DGCR8 binding ability to pri-miR199 in MCF7 cells before and after fulvestrant treatment. F. RIP analysis of m6A modification of pri-miR199. G. RIP analysis of DGCR8 binding ability to pri-miR199 in MCF7 cells before and after siMETTL3 treatment. H. Real-time PCR analysis of pri-miR199, pre-miR199, and mature miR199a-5p expression in MCF7 cells before and after siMETTL3 treatment. I. RIP analysis of pri-miR199 m6A modification in MCF7 cells before and after fulvestrant treatment. J. RIP analysis of METTL3 binding ability to pri-miR199 in MCF7 cells before and after fulvestrant treatment. K. RIP analysis of ERα binding ability to pri-miR199. L. RNA-pull down analysis of the interaction of pri-miR199 with METTL3 and ERα.

8C and S7D), alongside increased apoptosis and decreased Ki67 expression (**Figure 8D**, **8E**). Notably, CAV1 expression was negatively correlated with ERα expression in xenograft tumor tissues (Figure S7E). Crucially, ERα+ breast cancer patients receiving fulvestrant plus nab-paclitaxel exhibited a Partial Response with significantly reduced target lesion sizes (**Figure 8F**, **8G**). Taken together, these results indicate that fulvestrant synergistically enhances the efficacy of Nab-Paclitaxel in ER+ breast cancer.

Discussion

Estrogen receptors (ER) play a critical role in the development and progression of breast cancers. However, ER+ breast cancers exhibit low sensitivity to chemotherapy, and the associated survival benefit from chemotherapy is limited [23, 24]. Overcoming chemoresistance remains a pressing need for ER+ breast cancer. The combination of endocrine therapy with chemotherapy is controversial, as tamoxifen may antagonize chemotherapeutic agents due to its estrogen-like agonist activity [25]. In contrast, fulvestrant, an ER-selective inhibitor, overcomes the disadvantages associated with tamoxifen, including its estrogen-like agonist activity, and also downregulates ER expression [23]. Previous studies have reported that ERα mediates chemotherapy resistance by inhibiting cell apoptosis and that fulvestrant synergizes with cytotoxic agents such as doxorubicin, paclitaxel, docetaxel, vinorelbine, and 5-fluorouracil in breast cancer [26]. However, the potential of ERα inhibition to enhance the effects of nab-paclitaxel has not yet been explored. Our study demonstrates that targeting ERα can significantly augment the efficacy of nab-paclitaxel in ER+ breast cancer, thereby expanding the repertoire of chemotherapeutic agents that can be combined with fulvestrant-based endocrine therapy. However, it's a pity that we just have used xenograft model but not generate PDX models to add more solid evidence in this research, we will still try PDX model for subsequent studies.

CAV1 is a membrane invagination protein involved in endocytosis of albumin-bound or conjugated chemotherapeutics. Gemcitabine upregulates CAV1 expression, imparting survival advantages to nab-paclitaxel treatment [27]. Similarly, we found that fulvestrant synergizes with nab-paclitaxel by restoring CAV1 expression. Consequently, CAV1 serves as a biomarker for predicting nab-paclitaxel response and tailoring treatments to the appropriate patient subset.

Protein translation is a complicated process influenced by multiple factors. For example, m6A modification facilitates the translation of heat shock factor 1 (HSF1) [17], while promoting the degradation of LncRNA AS-ARHGAP5 [28]. Our current study shows that ERα also restricts m6A modification and translation efficiency of CAV1 mRNA, adding a layer of complexity to m6A-regulated RNA fates. We also found that miR199a-5p targets CAV1 mRNA and inhibits translation, which is consistent with previous reports [29]. Thus, we propose that ERα suppresses CAV1 translation by influencing the competitive interplay between the miR199a-5p interaction and m6A modification of CAV1 mRNA.

Regulation of miRNA maturation has been gaining widespread attention recently, given the functional significance of miRNAs in numerous diseases [30]. Generally, miRNA biogenesis involves three steps. First, long primary miRNA (pri-miRNA) transcripts with a stem loop hairpin structure are encoded by miRNA genes, which are transcribed by RNA Polymerase II or III. This process predominantly involves the interplay of genomic cis-regulatory elements with trans-

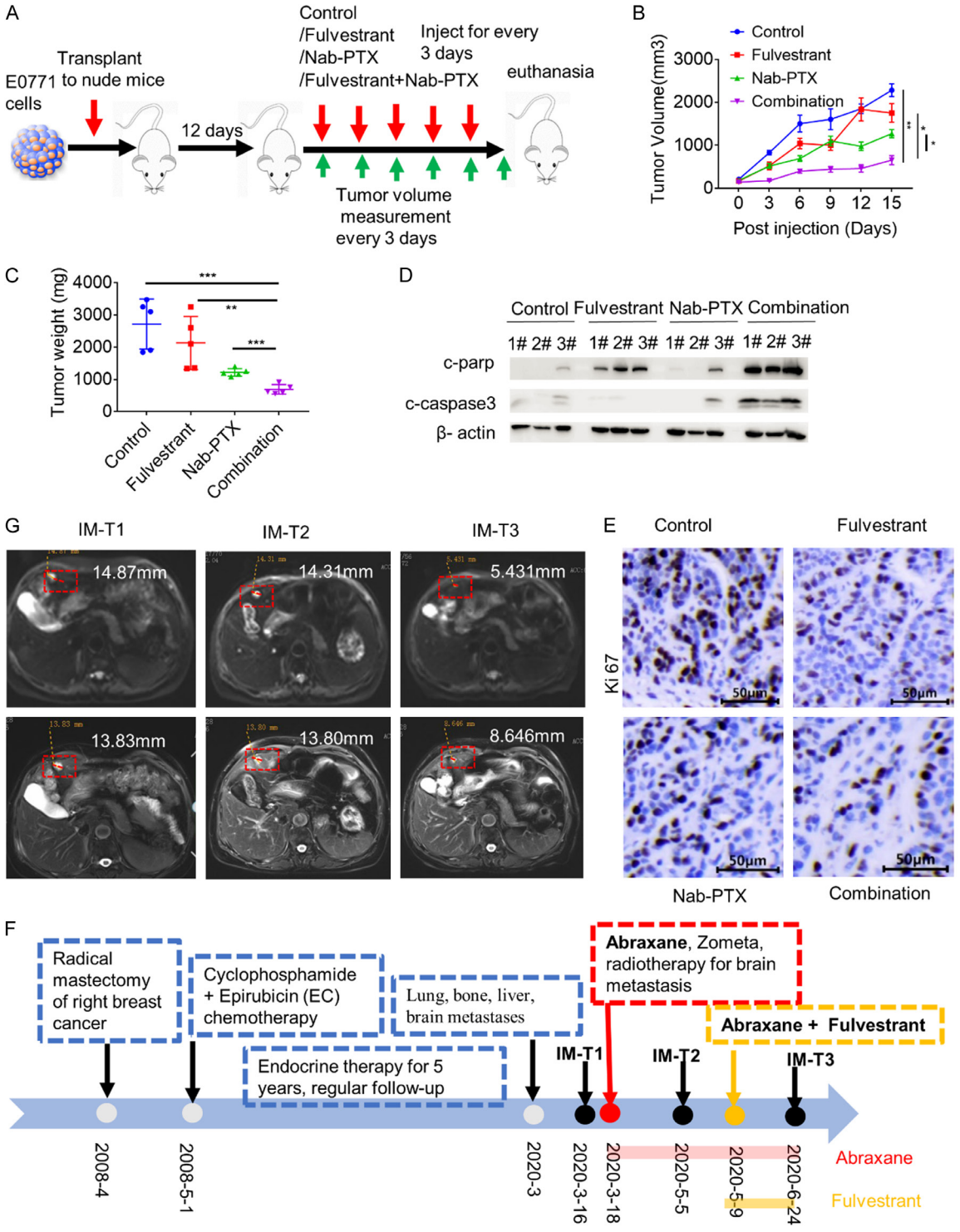

Figure 8. Fulvestrant has a synthetic lethal with Nab-Paclitaxel in vivo. A. Animal Experiment schematic diagram: nude mice were randomized to treatment with control, fulvestrant alone (2.5 mg/kg), nab-paclitaxel alone (22.3 mg/kg) or fulvestrant plus nab-paclitaxel. B. Dynamic tumor growth. C. Weight of tumors. D. Western blot analysis of c-parp and c-caspase3 protein expression. E. IHC analysis of Ki-67 protein expression. F. Clinical patient therapeutic schedule. G. Radiology showing a decrease in the target lesion diameter after treatment.

factors, including transcription factors, co-activators, co-repressor complexes, and chromatin modifications [31]. Second, pri-miRNAs are cleaved to generate hairpin intermediates (pre-

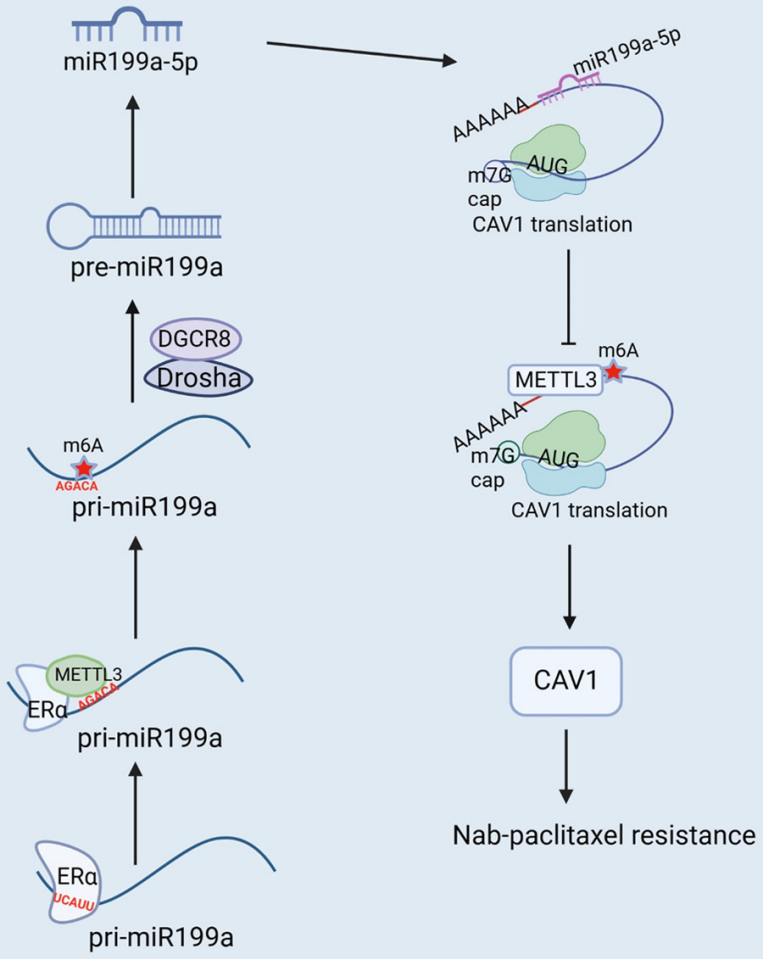

Figure 9. ERα recruits METTL3 to write m6A in pri-miR199a and promotes its maturation, which antagonize m6A modification of CAV1 mRNA to inhibit its translation, leading Nab-paclitaxel resistance.

miRNAs) by the microprocessor complex comprised of RNase III Drosha and its obligate RNA-binding protein partner, DiGeorge syndrome critical region gene (DGCR8). Pre-miRNAs are then exported from the nucleus to the cytoplasm by Exportin 5. Third, pre-miRNAs are processed into short-lived double-stranded duplexes by cytoplasmic RNase III Dicer, which employs the RNA-binding cofactor TAR RNA-binding protein (TRBP). These duplexes are then separated, with one strand selected as the mature miRNA and the other rapidly degraded. Regulators of miRNA processing bind to the stem or loop regions of miRNA precursors, influencing their processing via Drosha and/or Dicer. For example, hnRNPA1 binds to a conserved region of the pri-miR-18a loop and promotes its cleavage by Drosha [32]. Similarly, KSRP binds to sequences in the loop region of several miRNA precursors and recruits Drosha and Dicer to the pri- and pre-miRNA, respectively, enhancing their processing [33]. In our study, we discovered that ERα promotes m6A-dependent maturation of pri-miR199 by facilitating its m6A modification, crucial for DGCR8 recruitment and effective processing. Our findings highlight an overlooked function of ER in the post-transcriptional regulation of RNA modification and miRNA maturation.

In summary, our study delineates a previously unrecognized nab-paclitaxel resistance mechanism in ER+ breast cancer, where ERα stimulates m6A-dependent miR199a-5p maturation to antagonize m6A modification and compromise translation of CAV1 mRNA (**Figure 9**). Importantly, we provide compelling preclinical and clinical evidence that combining the ERα inhibitor fulvestrant with nab-paclitaxel offers a synergistic therapeutic strategy for ER-positive breast cancer.

Acknowledgements

This work was supported by grant from Zhejiang Provincial Natural Science Foundation of China under Grant No. LD21H160001 to J.H., Zhejiang Natural Science Foundation to Dr. Xian Wang (LD22H160003), Science and Technology Project of Jinhua, Zhejiang Province (2023-3-030), and Zhejiang Province Medical and Health Science and Technology Program (2020KY597). We thank members of our laboratories for their suggestions.

All the patients had signed the informed consent.

Disclosure of conflict of interest

None.

Address correspondence to: Xian Wang, Department of Medical Oncology, Sir Run Run Shaw

Hospital, School of Medicine, Zhejiang University, No. 3 Qinchun East Road, Hangzhou 310016, Zhejiang, China. E-mail: wangx118@zju.edu.cn; Hongchuan Jin, Biomedical Research Center, Sir Run Run Shaw Hospital, School of Medicine, Zhejiang University, No. 3 Qinchun East Road, Hangzhou 310016, Zhejiang, China. Tel: +86-13456726060; E-mail: jinhc@zju.edu.cn

References

[1] Siersbæk R, Kumar S and Carroll JS. Signaling pathways and steroid receptors modulating estrogen receptor α function in breast cancer. Genes Dev 2018; 32: 1141-1154.

[2] Early Breast Cancer Trialists' Collaborative Group (EBCTCG), Davies C, Godwin J, Gray R, Clarke M, Cutter D, Darby S, McGale P, Pan HC, Taylor C, Wang YC, Dowsett M, Ingle J and Peto R. Relevance of breast cancer hormone receptors and other factors to the efficacy of adjuvant tamoxifen: patient-level meta-analysis of randomised trials. Lancet 2011; 378: 771-784.

[3] Musgrove EA and Sutherland RL. Biological determinants of endocrine resistance in breast cancer. Nat Rev Cancer 2009; 9: 631-643.

[4] Von Hoff DD, Ervin T, Arena FP, Chiorean EG, Infante J, Moore M, Seay T, Tjulandin SA, Ma WW, Saleh MN, Harris M, Reni M, Dowden S, Laheru D, Bahary N, Ramanathan RK, Tabernero J, Hidalgo M, Goldstein D, Van Cutsem E, Wei X, Iglesias J and Renschler MF. Increased survival in pancreatic cancer with nab-paclitaxel plus gemcitabine. N Engl J Med 2013; 369: 1691-1703.

[5] Gradishar WJ, Tjulandin S, Davidson N, Shaw H, Desai N, Bhar P, Hawkins M and O'Shaughnessy J. Phase III trial of nanoparticle albumin-bound paclitaxel compared with polyethylated castor oil-based paclitaxel in women with breast cancer. J Clin Oncol 2005; 23: 7794-7803.

[6] Socinski MA, Bondarenko I, Karaseva NA, Makhson AM, Vynnychenko I, Okamoto I, Hon JK, Hirsh V, Bhar P, Zhang H, Iglesias JL and Renschler MF. Weekly nab-paclitaxel in combination with carboplatin versus solvent-based paclitaxel plus carboplatin as first-line therapy in patients with advanced non-small-cell lung cancer: final results of a phase III trial. J Clin Oncol 2012; 30: 2055-2062.

[7] Untch M, Jackisch C, Schneeweiss A, Conrad B, Aktas B, Denkert C, Eidtmann H, Wiebringhaus H, Kümmel S, Hilfrich J, Warm M, Paepke S, Just M, Hanusch C, Hackmann J, Blohmer JU, Clemens M, Darb-Esfahani S, Schmitt WD, Dan Costa S, Gerber B, Engels K, Nekljudova V, Loibl S and von Minckwitz G; German Breast Group (GBG); Arbeitsgemeinschaft Gynäkologische Onkologie-Breast (AGO-B) Investigators. Nab-paclitaxel versus solvent-based paclitaxel in neoadjuvant chemotherapy for early breast cancer (GeparSepto-GBG 69): a randomised, phase 3 trial. Lancet Oncol 2016; 17: 345-356.

[8] Chatterjee M, Ben-Josef E, Robb R, Vedaie M, Seum S, Thirumoorthy K, Palanichamy K, Harbrecht M, Chakravarti A and Williams TM. Caveolae-mediated endocytosis is critical for albumin cellular uptake and response to albumin-bound chemotherapy. Cancer Res 2017; 77: 5925-5937.

[9] Joglekar M, Elbezanti WO, Weitzman MD, Lehman HL and van Golen KL. Caveolin-1 mediates inflammatory breast cancer cell invasion via the Akt1 pathway and RhoC GTPase. J Cell Biochem 2015; 116: 923-933.

[10] Low JY and Laiho M. Caveolae-associated molecules, tumor stroma, and cancer drug resistance: current findings and future perspectives. Cancers (Basel) 2022; 14: 589.

[11] Schwartz LH, Seymour L, Litière S, Ford R, Gwyther S, Mandrekar S, Shankar L, Bogaerts J, Chen A, Dancey J, Hayes W, Hodi FS, Hoekstra OS, Huang EP, Lin N, Liu Y, Therasse P, Wolchok JD and de Vries E. RECIST 1.1 - standardisation and disease-specific adaptations: perspectives from the RECIST Working Group. Eur J Cancer 2016; 62: 138-145.

[12] Frost LS, Dhingra A, Reyes-Reveles J and Boesze-Battaglia K. The use of DQ-BSA to monitor the turnover of autophagy-associated cargo. Methods Enzymol 2017; 587: 43-54.

[13] Bartel DP. MicroRNAs: genomics, biogenesis, mechanism, and function. Cell 2004; 116: 281-297.

[14] Fabian MR and Sonenberg N. The mechanics of miRNA-mediated gene silencing: a look under the hood of miRISC. Nat Struct Mol Biol 2012; 19: 586-593.

[15] Fabian MR, Sonenberg N and Filipowicz W. Regulation of mRNA translation and stability by microRNAs. Annu Rev Biochem 2010; 79: 351-379.

[16] Liu T, Wei Q, Jin J, Luo Q, Liu Y, Yang Y, Cheng C, Li L, Pi J, Si Y, Xiao H, Li L, Rao S, Wang F, Yu J, Yu J, Zou D and Yi P. The m6A reader YTHDF1 promotes ovarian cancer progression via augmenting EIF3C translation. Nucleic Acids Res 2020; 48: 3816-3831.

[17] Song P, Feng L, Li J, Dai D, Zhu L, Wang C, Li J, Li L, Zhou Q, Shi R, Wang X and Jin H. β-catenin represses miR455-3p to stimulate m6A modification of HSF1 mRNA and promote its translation in colorectal cancer. Mol Cancer 2020; 19: 129.

[18] Alarcón CR, Goodarzi H, Lee H, Liu X, Tavazoie S and Tavazoie SF. HNRNPA2B1 is a mediator of m(6)A-dependent nuclear RNA processing events. Cell 2015; 162: 1299-1308.
[19] Alarcón CR, Lee H, Goodarzi H, Halberg N and Tavazoie SF. N6-methyladenosine marks primary microRNAs for processing. Nature 2015; 519: 482-485.
[20] Zhang J, Bai R, Li M, Ye H, Wu C, Wang C, Li S, Tan L, Mai D, Li G, Pan L, Zheng Y, Su J, Ye Y, Fu Z, Zheng S, Zuo Z, Liu Z, Zhao Q, Che X, Xie D, Jia W, Zeng MS, Tan W, Chen R, Xu RH, Zheng J and Lin D. Excessive miR-25-3p maturation via N(6)-methyladenosine stimulated by cigarette smoke promotes pancreatic cancer progression. Nat Commun 2019; 10: 1858.
[21] Carrasco E, Garrido JM, Álvarez PJ, Álvarez-Manzaneda E, Chahboun R, Messouri I, Melguizo C, Aránega A and Rodríguez-Serrano F. Meroxest improves the prognosis of immunocompetent C57BL/6 mice with allografts of E0771 mouse breast tumor cells. Arch Med Sci 2016; 12: 919-927.
[22] Gu JW, Young E, Patterson SG, Makey KL, Wells J, Huang M, Tucker KB and Miele L. Postmenopausal obesity promotes tumor angiogenesis and breast cancer progression in mice. Cancer Biol Ther 2011; 11: 910-917.
[23] Sui M, Huang Y, Park BH, Davidson NE and Fan W. Estrogen receptor α mediates breast cancer cell resistance to paclitaxel through inhibition of apoptotic cell death. Cancer Res 2007; 67: 5337-5344.
[24] Berry DA, Cirrincione C, Henderson IC, Citron ML, Budman DR, Goldstein LJ, Martino S, Perez EA, Muss HB, Norton L, Hudis C and Winer EP. Estrogen-receptor status and outcomes of modern chemotherapy for patients with node-positive breast cancer. JAMA 2006; 295: 1658-1667.
[25] Hug V, Hortobagyi GN, Drewinko B and Finders M. Tamoxifen-citrate counteracts the antitumor effects of cytotoxic drugs in vitro. J Clin Oncol 1985; 3: 1672-1677.
[26] Ikeda H, Taira N, Nogami T, Shien K, Okada M, Shien T, Doihara H and Miyoshi S. Combination treatment with fulvestrant and various cytotoxic agents (doxorubicin, paclitaxel, docetaxel, vinorelbine, and 5-fluorouracil) has a synergistic effect in estrogen receptor-positive breast cancer. Cancer Sci 2011; 102: 2038-2042.
[27] Borsoi C, Leonard F, Lee Y, Zaid M, Elganainy D, Alexander JF, Kai M, Liu YT, Kang Y, Liu X, Koay EJ, Ferrari M, Godin B and Yokoi K. Gemcitabine enhances the transport of nanovector-albumin-bound paclitaxel in gemcitabine-resistant pancreatic ductal adenocarcinoma. Cancer Lett 2017; 403: 296-304.
[28] Zhu L, Zhu Y, Han S, Chen M, Song P, Dai D, Xu W, Jiang T, Feng L, Shin VY, Wang X and Jin H. Impaired autophagic degradation of lncRNA ARHGAP5-AS1 promotes chemoresistance in gastric cancer. Cell Death Dis 2019; 10: 383.
[29] Du F, Zhang Y, Xu Q, Teng Y, Tao M, Chen AF and Jiang R. Preeclampsia serum increases CAV1 expression and cell permeability of human renal glomerular endothelial cells via down-regulating miR-199a-5p, miR-199b-5p, miR-204. Placenta 2020; 99: 141-151.
[30] Volinia S, Calin GA, Liu CG, Ambs S, Cimmino A, Petrocca F, Visone R, Iorio M, Roldo C, Ferracin M, Prueitt RL, Yanaihara N, Lanza G, Scarpa A, Vecchione A, Negrini M, Harris CC and Croce CM. A microRNA expression signature of human solid tumors defines cancer gene targets. Proc Natl Acad Sci U S A 2006; 103: 2257-2261.
[31] Chang TC, Zeitels LR, Hwang HW, Chivukula RR, Wentzel EA, Dews M, Jung J, Gao P, Dang CV, Beer MA, Thomas-Tikhonenko A and Mendell JT. Lin-28B transactivation is necessary for Myc-mediated let-7 repression and proliferation. Proc Natl Acad Sci U S A 2009; 106: 3384-3389.
[32] Guil S and Cáceres JF. The multifunctional RNA-binding protein hnRNP A1 is required for processing of miR-18a. Nat Struct Mol Biol 2007; 14: 591-596.
[33] Trabucchi M, Briata P, Garcia-Mayoral M, Haase AD, Filipowicz W, Ramos A, Gherzi R and Rosenfeld MG. The RNA-binding protein KSRP promotes the biogenesis of a subset of microRNAs. Nature 2009; 459: 1010-1014.

Table S1. RNA oligonucleotide sequences

Primers	
Name	Sequence
Actin	F: CACCAACTGGGACGACAT
	R: ACAGCCTGGATAGCAACG
CAV1	F: ATGTCTGGGGGCAAATACGTA
	R: GTTGAGGTGTTTAGGGTCGC
miR199a-5p	F: CCCAGTGTTCAGACTACCTGTTC
	R: universal primer
miR199 primary	F: AGTGGTGGTTTCCTTGGCT
	R: GGGGCCGGCTATCCATCC
miR199 precursor	F: GCCAACCCAGTGTTCAGACT
	R: universal primer
pri-miR199 transcript	F: AGTGGTGGTTTCCTTGGCTG
	R: TTCTATGCGAGGCTCTGCCA
miRNAs mimics and inhibitors	
NC mimic	S: UUCUCCGAACGUGUCACGUTT
	AS: ACGUGACACGUUCGGAGAATT
miR199a-5p mimic	S: CCCAGUGUUCAGACUACCUGUUC
	AS: ACAGGUAGUCUGAACACUGGGUU
Inhibitor NC	S: CAGUACUUUUGUGUAGUACAA
miR-493-3p inhibitor	S: CCUGGCACACAGUAGACCUUCA
miR-520a-3p inhibitor	S: ACAGUCCAAAGGGAAGCACUUU
miR-124-3p inhibitor	S: UUGGCAUUCACCGCGUGCCUUA
miR-302b-3p inhibitor	S: CUACUAAAACAUGGAAGCACUUA
miR-384 inhibitor	S: UAUGAACAAUUUCUAGGAAU
miR-199a-5p inhibitor	S: GAACAGGUAGUCUGAACACUGGG
siRNAs	
Control siRNA	S: UUCUCCGAACGUGUCACGUTT
	AS: ACGUGACACGUUCGGAGAATT
CAV1-1	S: GCCGUGUCUAUUCCAUCUATT
	AS: UAGAUGGAAUAGACACGGCTT
CAV1-2	S: GCGACCCUAAACACCUCAATT
	AS: UUGAGGUGUUUAGGGUCGCTT
ESR1-1	S: GAGGGAGAAUGUUGAAACATT
	AS: UGUUUCAACAUUCUCCCUCTT
ESR1-2	S: GGUUCCGCAUGAUGAAUCUTT
	AS: AGAUUCAUCAUGCGGAACCTT
METTL3-1	S: GCAAGAAUUCUGUGACUAUTT
	AS: AUAGUCACAGAAUUCUUGCTT
METTL3-2	S: GCUGCACUUCAGACGAAUUTT
	AS: AAUUCGUCUGAAGUGCAGCTT

Table 1 Patients Baseline

Subtype	Number
ER-	30
ER+	55
Total	85

Figure S1. Lower response to Nab-paclitaxel in ER+ BC than ER- BC. Patients ER status Baseline.

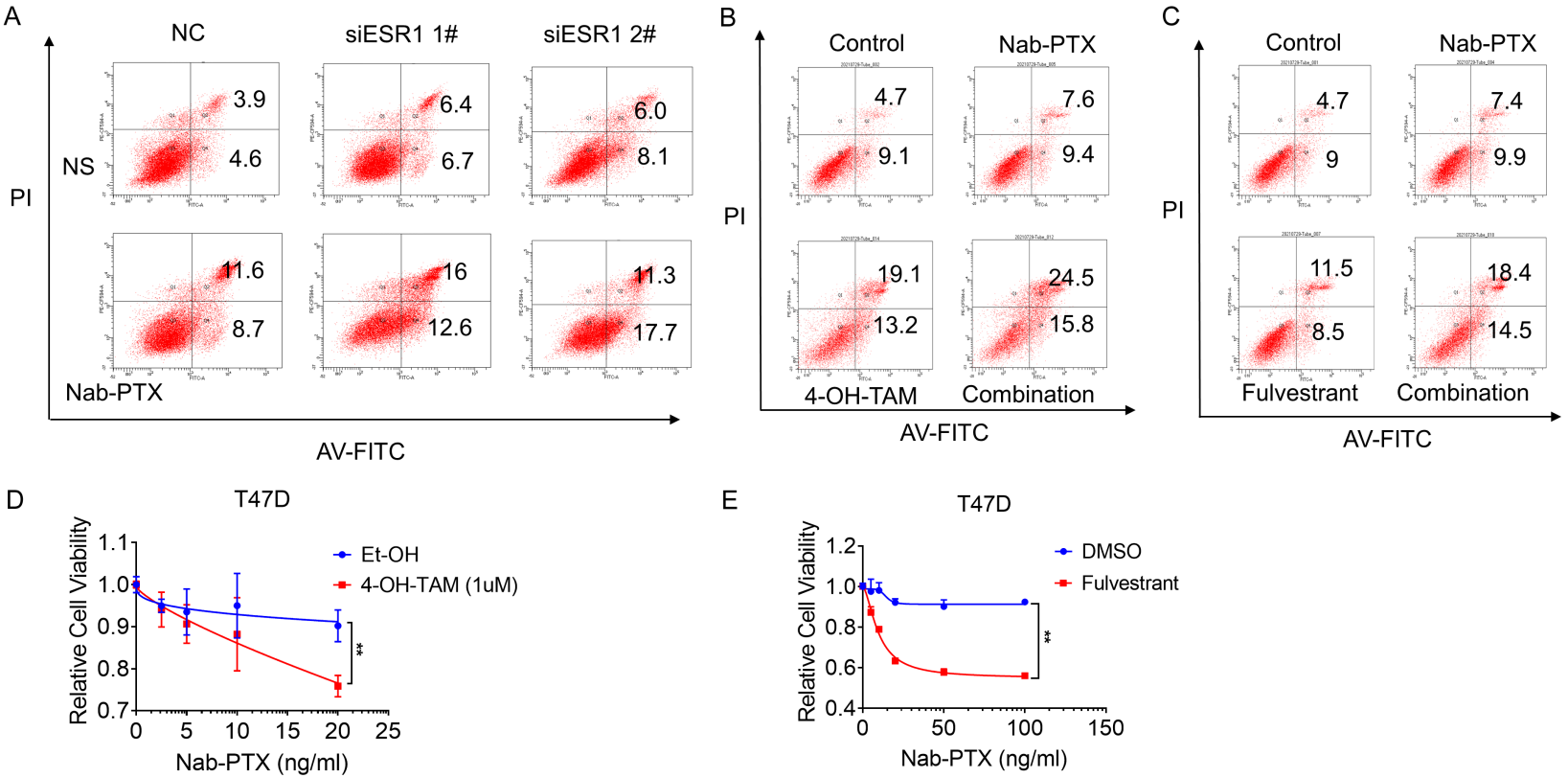

Figure S2. Inhibition of ERα enhance the sensitivity to Nab-paclitaxel in vitro. A. Analysis of cell viability after siESR1 with Nab-PTX in MCF7 cells using flow cytometry. B. Analysis of cell viability after combining 4-OH-TAM (5 uM) with Nab-PTX in MCF7 cells using flow cytometry. C. Analysis of cell viability after combining Fulvestrant (100 nM) with Nab-PTX in MCF7 cells using flow cytometry. D. Analysis of cell viability after combining 4-OH-TAM (1 uM) with Nab-PTX in T47D cells using MTS assay. E. Analysis of cell viability after combining Fulvestrant (100 nM) with Nab-PTX in T47D cells using MTS assay.

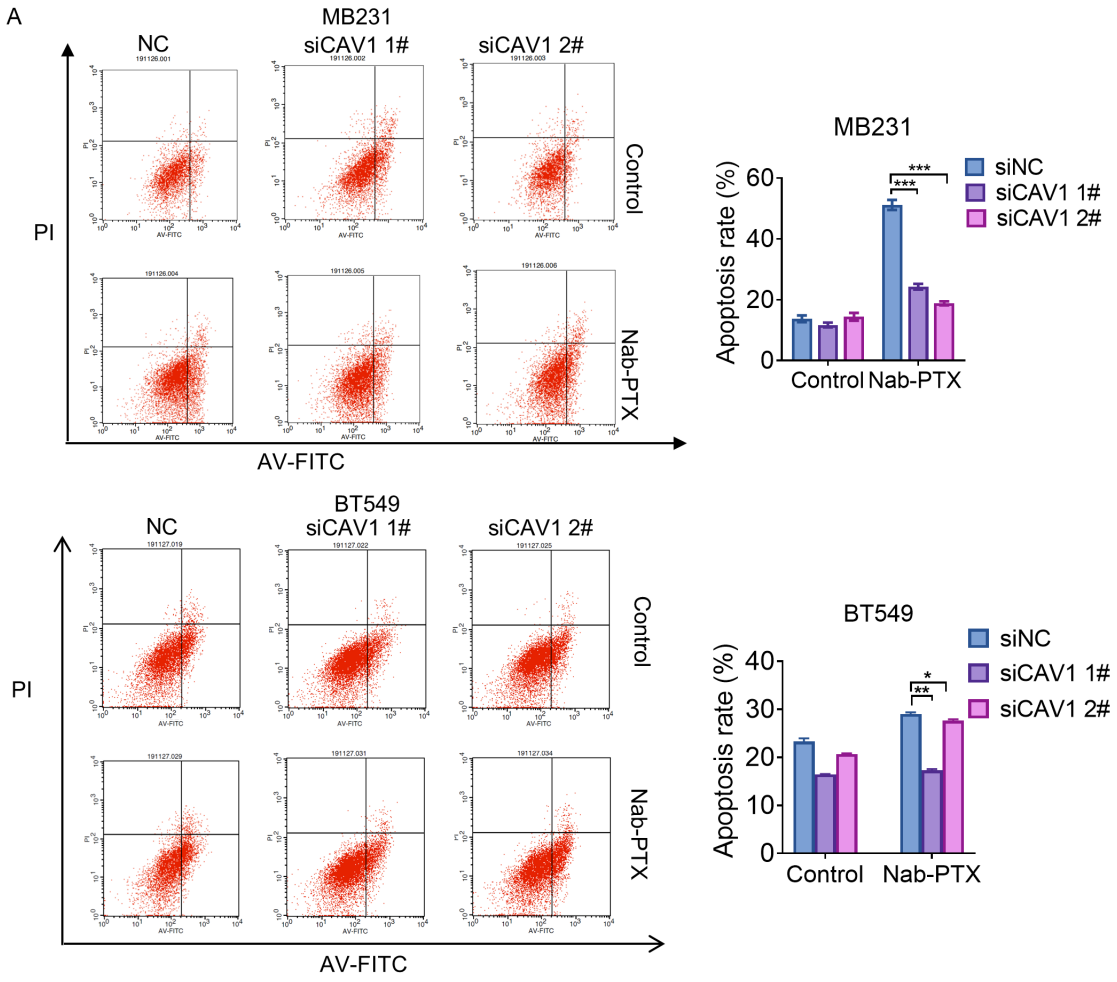
A
MB231
NC
siCAV1 1#
siCAV1 2#
Control
Nab-PTX
PI
AV-FITC
MB231
Apoptosis rate (%)
siNC
siCAV1 1#
siCAV1 2#
Control
Nab-PTX
BT549
BT549
B
MB231
siCAV1
NC1# 2# NC1# 2#
Nab-PTX
c-parp
CAV1
β-actin
BT549
C
BT549
Relative Cell Viability
Nab-PTX (ng/ml)
T47D
vector
CAV1
D
MCF7
E
MCF7
T47D

Figure S3. CAV1 is relevant to the sensitivity of breast cancer cells to Nab-paclitaxel. A. Analysis of apoptosis after siCAV1 with Nab-PTX (10 ng/ml) in MB231 and BT549 by flow cytometry. B. Analysis of apoptosis after siCAV1 with Nab-PTX (10 ng/ml) in MB231 and BT549 by Western blot. C. Analysis of cell viability after siCAV1 with Nab-PTX in BT549 by MTS assays. D. Analysis of cell viability after CAV1 overexpress with Nab-PTX in MCF7 and T47D by MTS. E. Analysis of apoptosis after CAV1 overexpress with Nab-PTX (10 ng/ml) in MCF7 and T47D by Western blot.

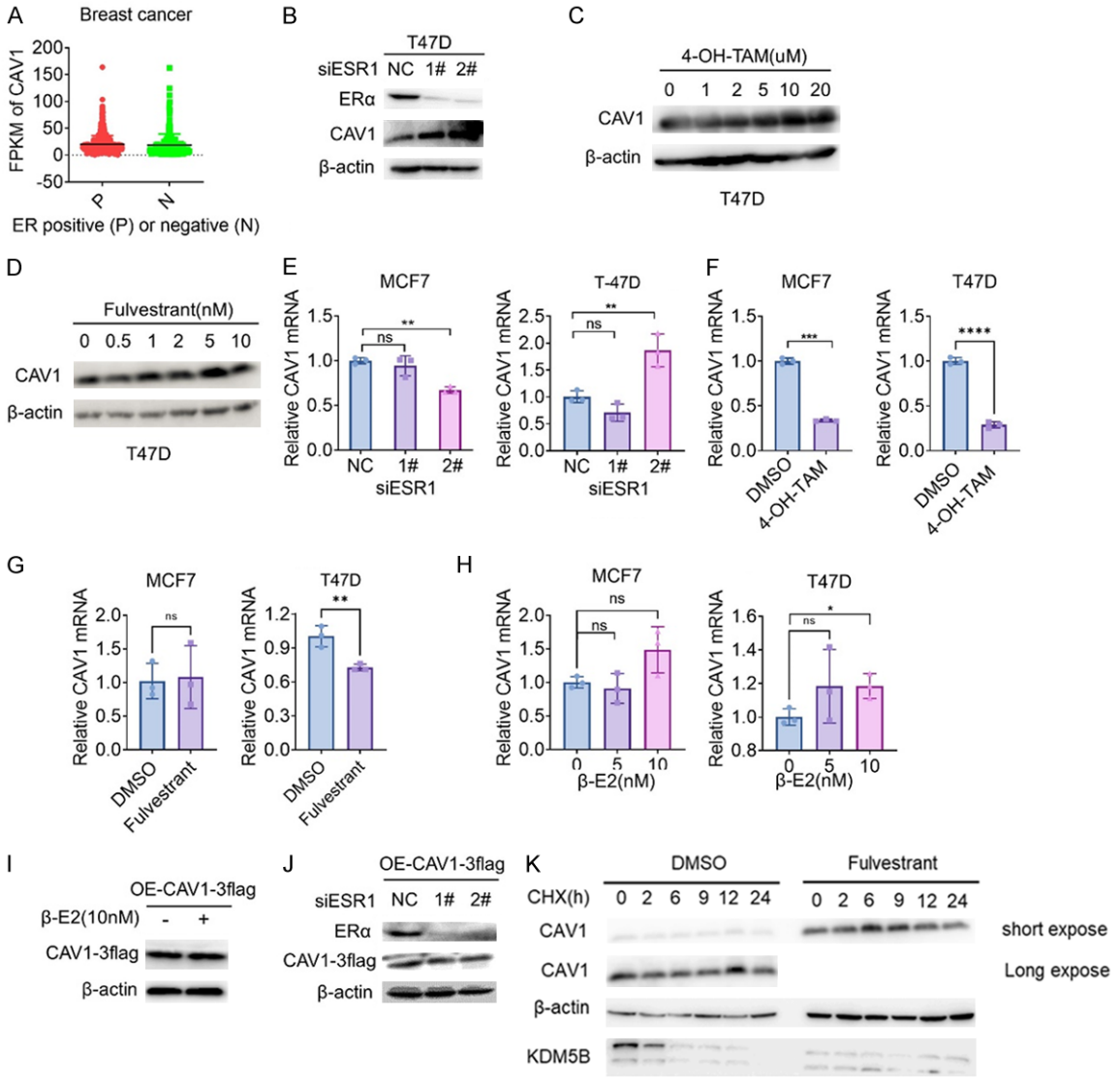

Figure S4. ERα downregulates CAV1 protein expression by inhibiting its translation. A. Correlation between ERα and CAV1 mRNA levels in BC tissues from TCGA. B. Western blot analysis CAV1 protein expression after siESR1 in T47D. C and D. Western blot analysis CAV1 protein expression after 4-OH-TAM, Fulvestrant in T47D. E-H. Real-time PCR analysis CAV1 mRNA expression after siESR1, 4-OH-TAM, Fulvestrant and β-E2. I and J. Western blot analysis exogenous CAV1 protein expression after β-E2 and siESR1. K. Cycloheximide (CHX) chase assay before and after Fulvestrant treatment.

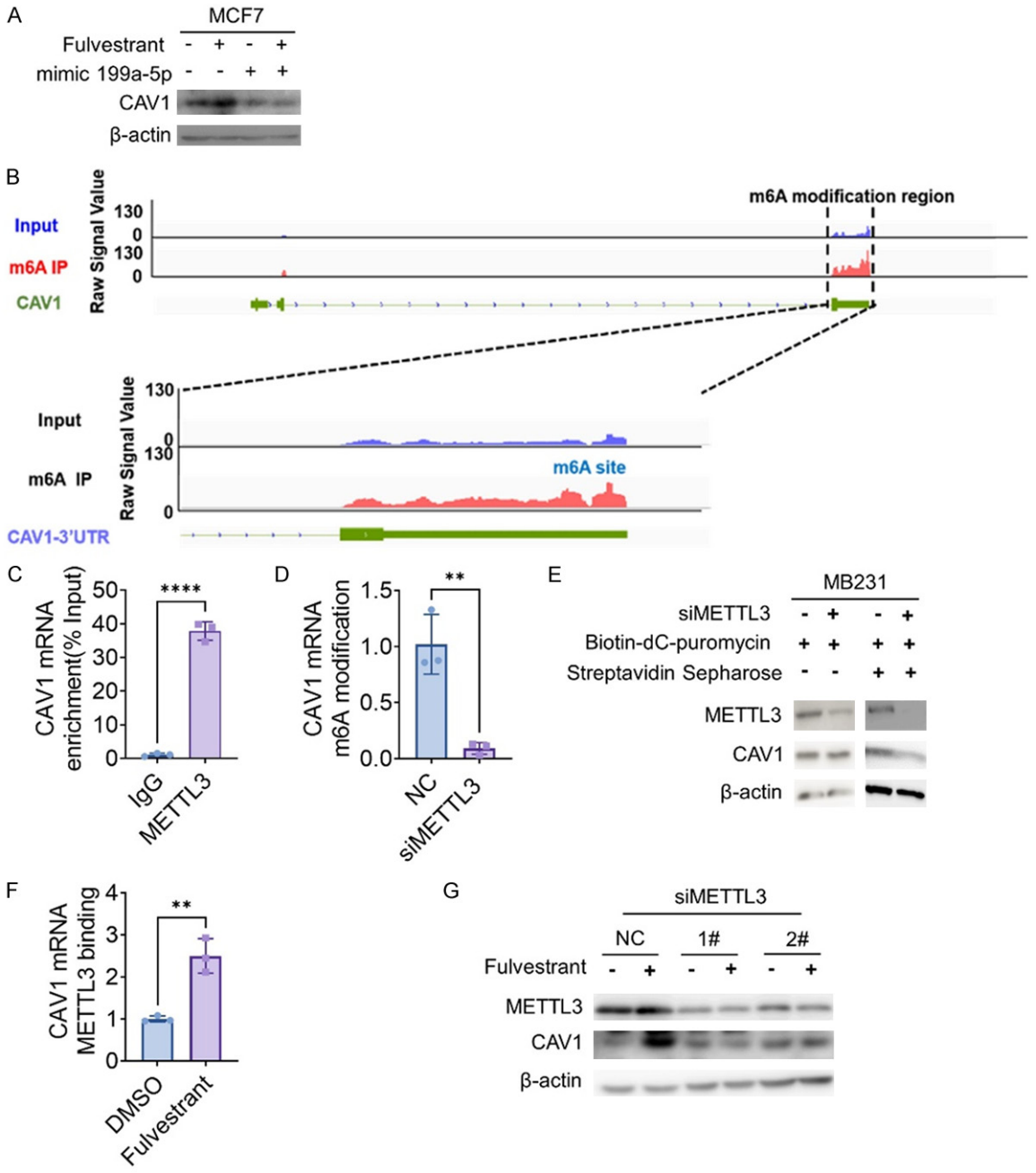

Figure S5. ERα promotes miR199a-5p to inhibit m6A modification of CAV1. A. Western blot analysis CAV1 expression after fulvestrant treatment and rescued by miR199a-5p mimic. B. meRIP-Seq revealed a hypermethylated peak in the 3'-UTR of CAV1 mRNA. C. RIP analysis METTL3 bind to CAV1 mRNA. D. RIP analysis CAV1 m6A level after siMETTL3. E. Puromycin-labelling test for CAV1 translation after siMETTL3. F. RIP analysis METTL3 bind to CAV1 mRNA after fulvestrant treatment. G. Western blot analysis CAV1 expression after fulvestrant treatment and rescued by siMETTL3.

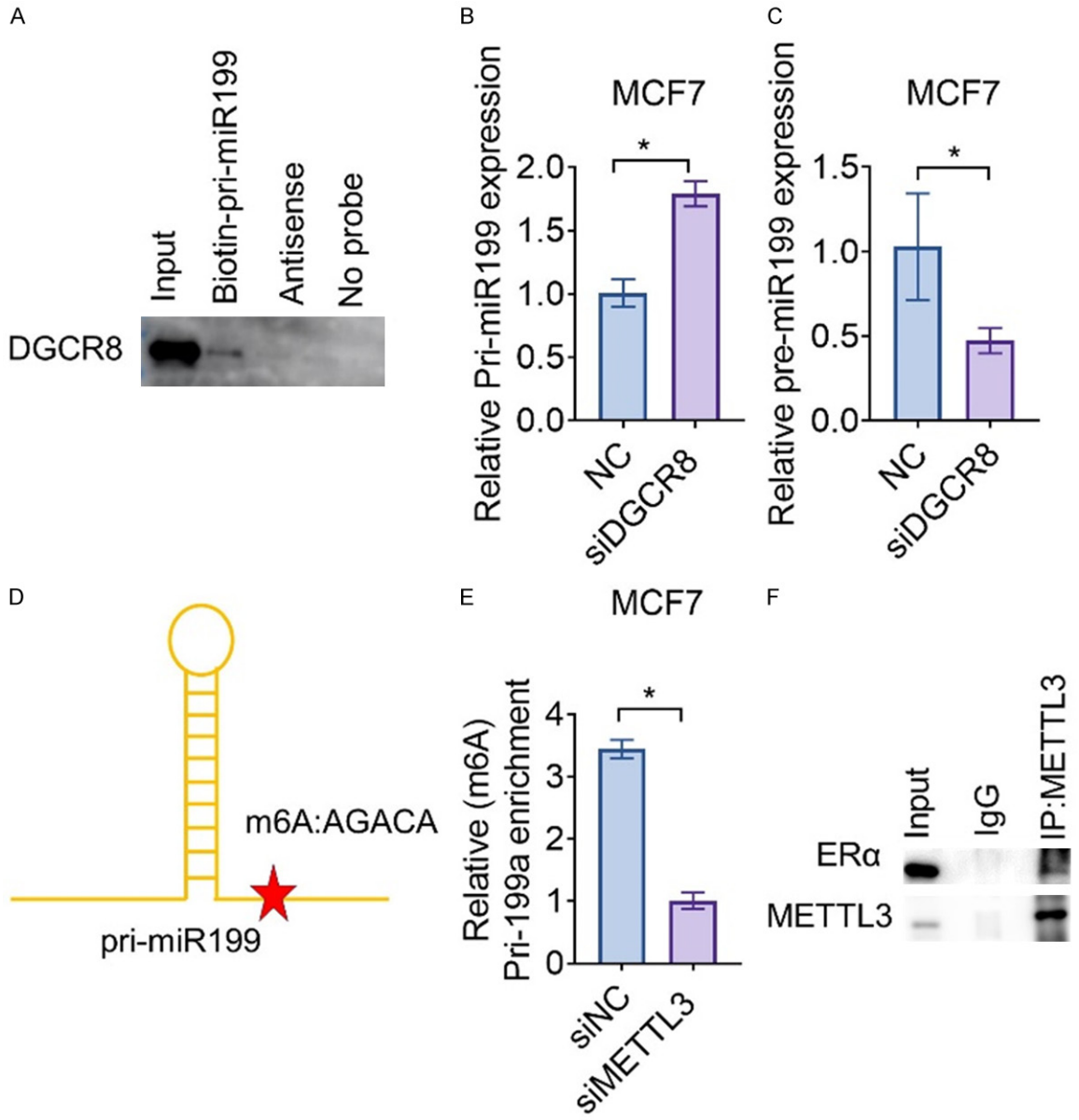

Figure S6. ERα promotes m6A-dependent maturation of miR199a-5p. A. RNA-pull down analysis of the interaction of pri-miR199 with DGCR8. B and C. Real-time PCR analysis of pri-miR199, pre-miR199 in MCF7 cells before and after siDGCR8 treatment. D. Diagram of m6A modification site in pri-miR199. E. RIP analysis pri-miR199 m6A level after siMETTL3. F. Co-IP shows ERα interact with METTL3.

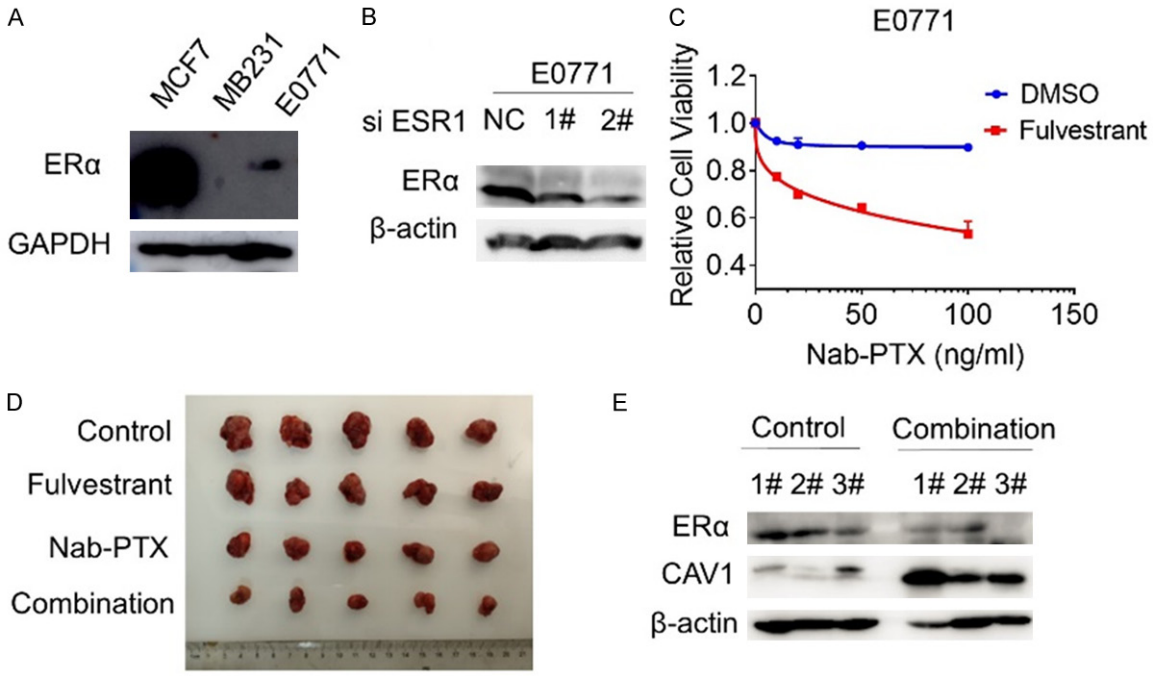

Figure S7. Fulvestrant has a synthetic lethal with Nab-Paclitaxel in vivo. A. Western blot analysis ERa expression in Eo771. B. Western blot analysis siESR1 knockdown efficacy. C. Analysis of cell viability after combine Fulvestrant (100 nM) with Nab-PTX in E0771 by MTS assays. D. Morphology of tumor. E. Western blot analysis CAV1 expression in tumor after combination Fulvestrant and Nab-PTX.